PROCEEDINGS, 47th Workshop on Geothermal Reservoir Engineering
Stanford University, Stanford, California, February 7-9, 2022
SGP-TR-223

Geothermal Cost Estimation Using Uncertainty and Flexible Design

R. Chadwick Holmes[1*†], Aimé Fournier[1], Richard de Neufville[1]

[1]Massachusetts Institute of Technology, Cambridge, MA 02139 USA,

[†]Currently at: Chevron Technical Center, Houston, TX 77002 USA,

[*]Correspondence: chadwick@alum.mit.edu

Keywords: techno-economic model, NPV, uncertainty, flexible design, decision rules, electricity, optimization, EGS, power plant

ABSTRACT

Geothermal techno-economic models currently in widespread use do not provide the means to jointly account for parameter uncertainties, dynamic operational strategies, and power-plant design flexibility in an integrated analysis. For available academic and government-provided tools, geothermal power generation cost estimates typically start with single-value inputs, although support for user-specified distributions capturing uncertainty in parameter values is becoming more commonplace. The missing piece in determining project value is allowing for flexible responses to uncertainties, where early architectural choices enable future conditions-based design modifications, and rules simulate field-management decisions made during the lifetime of a plant. This paper proposes a different template for estimating power-project value that incorporates design flexibility. First, the static model is defined with deterministic parameter inputs. Significant uncertainties like the initial subsurface conditions, variation in the local environment over time, and broader risks like disruptions to the electricity market from national electrification, are evaluated through a sensitivity analysis. The most sensitive features are assigned probability density functions, each sampled in repeated model runs to form a Monte Carlo solution ensemble. This base model is then enhanced with decision rules for executing design flexibilities. Multi-dimensional analysis of the final results provides decision-makers with insights into the optimal choice of facility design, construction timeline, and strategy among those tested that best mitigates the risk of poor economic outcomes for the geothermal investment. This study applies the proposed modeling approach to a hypothetical Enhanced Geothermal System (EGS) expansion of an existing plant in New Mexico. The modeled concept uses modular power-plant units targeting a shallow reservoir, offset from the hydrothermal system currently utilized for producing electricity. Each module comprises a single injector-producer pair connected to a binary cycle generator based on a present-day commercial system analog. The initial cost model provides a static assessment of capital expenses, operating and maintenance costs, and income from power sales to determine the Net Present Value (NPV) over the useful life of the plant. After supplementing key model parameters with probability distributions, the model uses multiple decision rules to adjust the plant design as operating conditions change over time. These rules are implemented in succession, defining scenarios with results ensembles compared using summary metrics, histograms, and target curves. Insights from the scenarios are enhanced by optimizing decision-rule threshold criteria, thereby characterizing a field-management strategy that maximizes upside potential without increasing downside risk.

1. INTRODUCTION

Academic scientists, government agencies, and energy companies regularly use cost models to predict the viability of commercial electricity generation from renewable resources. Geothermal production planning must rely on model-based estimates due to the few commercial analogs, particularly for unconventional geothermal development methods like advanced closed loop (ACL) and enhanced geothermal systems (EGS). Before the early 2000s, geothermal economic models focused on order-of-magnitude cost estimates of drilling and power-plant construction to identify optimal reservoir depths and design temperatures for a given geothermal gradient range (Tester & Herzog, 1990). With the release of "The Future of Geothermal Energy" report came the MIT EGS model, a cost-estimation tool using globally-derived empirical relationships for major project cost elements (Tester et al., 2006). This tool was rebranded "GEOthermal energy for the Production of Heat and electricity (IR, standing for current × resistance) Economically Simulated" (GEOPHIRES) after several upgrades, including support for direct use and cogeneration applications (Beckers et al., 2013). The latest version of GEOPHIRES (v2.0), released as open-source Python code, accepts a set of deterministic input parameters grouped into five categories: subsurface, surface, financial, capital and operations & maintenance costs, and simulation parameters, to predict a levelized cost of electricity (LCOE) when estimating power generation (Beckers & McCabe, 2018, 2019)

The primary alternative to GEOPHIRES is the Geothermal Electric Technology Evaluation Model (GETEM), a spreadsheet model that determines LCOE for commercial power production. GETEM was created for the National Renewable Energy Laboratory (NREL) as a tool for prioritizing geothermal projects and testing the economic impact of technology improvements (Entingh et al., 2006). An upgrade in 2011 included support for EGS reservoirs (EERE, 2012). Although the workbook format makes GETEM customizable, general users may find its multitude of worksheets and complex cross-references overwhelming. Furthermore, password protections lock down many of the sheets from full visibility or editing. GETEM offers a tremendous number of user inputs, all deterministic in nature. The main cost components in the model include exploration, drilling and stimulation, well and reservoir management, and power-plant construction and maintenance (Entingh et al., 2006). As with GEOPHIRES, GETEM does not natively support probabilistic modeling or dynamic decision-making in the cost simulation.

NREL elected to include GETEM logic in the System Advisor Model (SAM) for multiple renewable energy systems, available online and as a downloadable application (NREL, 2021b). SAM goes beyond power sales to a utility, modeling residential projects to offset electricity needs and third-party ownership arrangements (Blair et al., 2018). SAM is also open-source, but since the majority of the code was written

in PowerBuilder and C++, incorporating custom logic or strategic decisions into cost calculations requires at least a moderate level of software-development proficiency. Uniquely, SAM supports Monte Carlo simulation with multi-valued input variables for stochastic and sensitivity analyses.

While not exhaustive, this survey of geothermal economic models illustrates the breadth of tools available for determining power-project feasibility for hydrothermal or EGS developments. Uncertainty is often not considered in a single model run. Instead, the user parameterizes the resource and power generation scenario to calculate a single cost estimate. Sensitivity testing or parameter ranges must be handled manually (except with SAM), and the models are largely incompatible with dynamic strategic decision-making over the lifetime of a field. The absence of these features defines an opportunity for a different modeling approach that accounts for uncertainty and allows for flexibility in the system design.

Incorporating flexible options in engineering designs offers a simple and elegant method for moving beyond sensitivity analysis of critical uncertainties into evaluating how uncertainty mitigation can lead to better project plans. Defining design options requires broader thinking about system interactions, stepping away from the strict bounds of a cost model being constructed to consider the assumptions underlying the model. For example, electricity forecasts from agencies like the U.S. Energy Information Agency (EIA) may appear foolproof, but a review of past Annual Energy Outlook (AEO) model projections (EIA, 2021b) shows just how frequently those forecasts miss the mark (Figure 1). Treating forecasts as deterministic ground truth would not only be factually incorrect, but it could also miss an opportunity for engineering solutions that can respond to deviations from average forecasted behavior to the benefit of operators and investors. Put differently, power-plant designs built on the assumptions of geothermal capacity needs depicted in the AEO10 and AEO20 curves in Figure 1 would not be the same, but adding flexibility can add responsiveness to the project, simultaneously optimizing for either scenario.

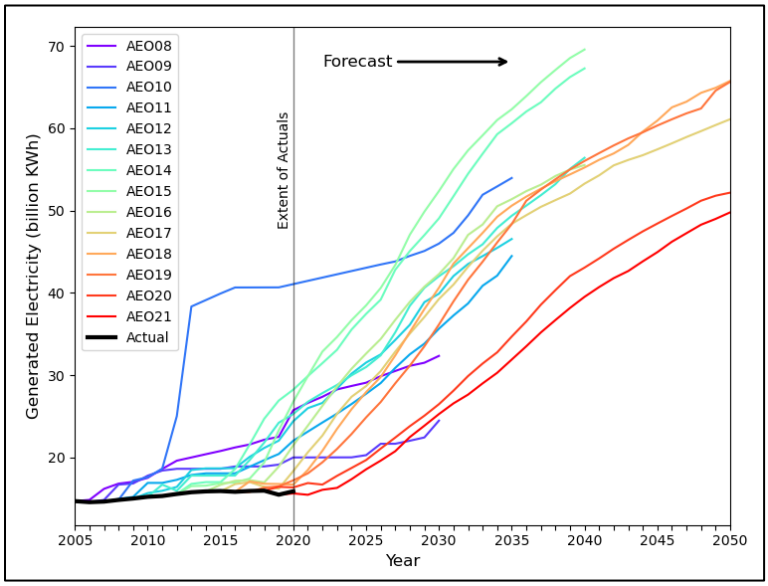

Figure 1: Actual electricity generation from geothermal sources by year (black line) and future projections (colored lines) from the EIA Annual Energy Outlook. Each projection represents a complex forecast based on numerous assumptions, including technology improvements in the production, distribution, and consumption of energy and an unchanging regulatory environment for the duration of the forecasted period. The release year of each prediction is noted in the legend.

Well-established geothermal cost models like GETEM present a highly-parameterized but deterministic view of cost and investment opportunity given a defined geothermal resource and development concept. Other models may apply different assumptions or mathematical treatments for various facets of the system; however, they uniformly offer a single-track aspect to how the project unfolds over its lifecycle. Users can test ideas, but the solution space remains under-explored due to implicit assumptions of variable trends or stases for what is a highly dynamic system.

In our proposed spreadsheet-based economic model outlined below, the analysis accounts for uncertainty by replacing single-value estimates with distributions for model variables. This enables the model to produce a representative range of possible outcomes when simulated many times over. In addition, flexibility analysis demonstrates the effect of intelligent system management where design options are executed in response to changing conditions. Designs need not be static, and testing flexibilities can significantly increase the expected value of a project by exploring execution strategies otherwise missed by more traditional modeling approaches (de Neufville & Scholtes, 2011, Chapter 6). In addition, the use of a simple spreadsheet form factor makes our model both accessible and straightforward to use for a creative exploration of power-plant concepts and operational strategies.

2. EGS EXPANSION CASE STUDY

We illustrate our proposed methodology by applying it to a hypothetical case study based on the Dale Burgett Geothermal plant, which we refer to as "Lightning Dock" due to the historical familiarity of that name. Lightning Dock is presently the sole commercial power plant operating in New Mexico. The net generating capacity started at 4 MW after the first development phase in 2013. An expected

second-phase upgrade to 10 MW never came to fruition. Instead, the facility underwent a significant refit in 2018, resulting in a net capacity of 11.2 MW generated entirely from hydrothermal brine production (Bonafin et al., 2019).

DOE-funded efforts to characterize the geothermal resources of the Animas Valley —where Lightning Dock is located— revealed two thermal reservoirs: the hydrothermal resource targeted by Lightning Dock, where deep geothermal fluids ascend along the Animas Valley Fault complex to ≈ 365-1000 m depth, and a secondary interval at ≈ 900–1200 m depth that requires permeability enhancement for production (Schochet & Cunniff, 2001). The second reservoir comprises the Horquilla limestone formation, estimated to span a minimum volume of 6 km³ based on conservative figures. By one proprietary study completed in 2001 for Ormat, the Horquilla has a most-likely production potential of 9.3 MW and an 88% probability of exceeding 6 MW (Schochet & Cunniff, 2001).

A proposal in 2001 envisioned constructing a 6 MW hybrid power plant combining hydrothermal and EGS-sourced power generation (Schochet & Cunniff, 2001). The authors noted several benefits of pursuing EGS in this location:

- Relatively shallow resource equates to lower drilling costs
- EGS water requirements attainable from paired hydrothermal operations
- Low/no assessed environmental impact from geothermal operations
- Direct access to in-place transmission lines
- Opportunity for direct electricity sales to local users

As suggested by this list, conditions at Lightning Dock are highly favorable for an EGS commercial-scale proof-of-concept. In this techno-economic analysis, we revise the 2001 proposal to focus on a near-field EGS expansion that ties back to the existing Lightning Dock facility and targets the Horquilla reservoir. Stepping out from the hydrothermal zone in proximity to the Animas Valley Fault complex, thermal conditions settle to a background geothermal gradient between ≈ 80–120 K/km, based on boreholes TG 56-14 and TG 12-7 (Cunniff & Bowers, 2003) — high enough to support geothermal capture. We chose 5 MW as the initial EGS expansion goal in keeping with the proof-of-concept intent of the proposal and this analysis.

3. POWER PLANT FLEXIBILITY

In this study, modular binary organic Rankine cycle (ORC) or binary-cycle power plants enable geothermal power production design flexibility. Small-scale binary-cycle plants on the kilowatt to single-digit megawatt scale are well-suited for low-temperature electricity generation, with applications in low-grade industrial waste heat, maritime vessel operations, or renewable energy sources (Winther, 2018). Both Orcan Energy and Climeon provide trailer-size air-cooled modules (Figure 2) that can be combined to scale production needs (Climeon, 2021; Orcan Energy AG, 2021). We select the Climeon Power Block as an analog for modeling due to the availability of reference spec sheets, although the analysis described here could extend to any modular binary-cycle plant. A Power Block module combines seven individual 150 kW units to provide 1050 kW of generation capacity, using inlet fluid temperatures from 80–120 °C and flow rates of 10–35 kg/s (Climeon, 2021).

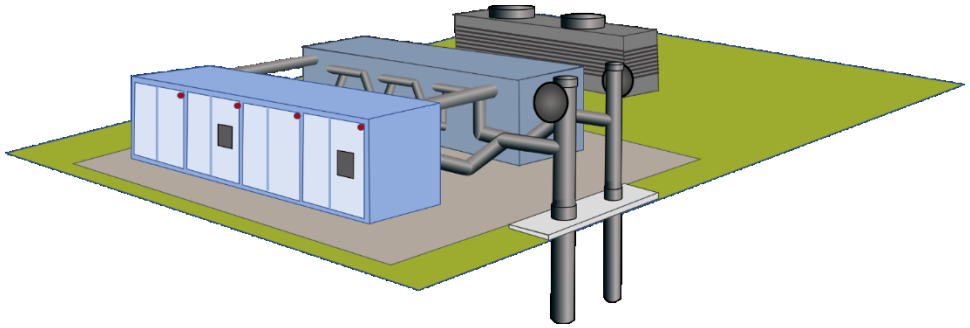

Figure 2: Modular binary cycle power plant concept, adapted from Climeon (Engman, 2018).

We define flexibility in our case study as the ability to add or shut down power-plant modules during the lifespan of the field. Using this strategy rather than constructing a fixed-capacity plant comes with an initial cost of flexibility, namely, that associated with the total land footprint potentially needed for power production. Delaying the acquisition of necessary rights could add years to a geothermal project (Young et al., 2019), discouraging any responsive decisions to install additional modules. Permitting and land access costs should count toward initial project capital expenses. However, our study does not include these costs because a 2500-acre geothermal lease already assigned to Lightning Dock (Thermal Zones, 2022) spans sufficient area for even the most aggressive expansion case that we consider.

4. METHODOLOGY

The cost-model methodology followed in this paper is outlined as a simplified workflow in Figure 3. In the first step, we create a static model for calculating the NPV of our proposed geothermal project, which required selecting important model parameters based on literature and industry sources. With a baseline deterministic estimate of NPV calculated, we construct a probabilistic model by selecting several uncertainties in the geothermal power system that could impact financial outcomes. We test model sensitivity to these uncertainties and characterize the most important ones with probability density functions (PDFs). In the last step, different operational strategies are defined using logical decision rules applied to the NPV calculation in each year of the project lifespan. The model then runs as a Monte Carlo simulation, building a histogram, cumulative distribution function or "target curve," and summary statistics for each strategy. These

simulation products provide multi-dimensional measures for strategy comparison and decision support for the design and execution of a geothermal project.

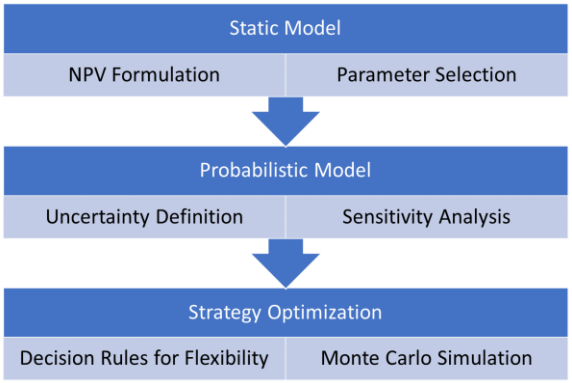

Figure 3: Workflow describing the cost model building process demonstrated by this study.

5. STATIC DISCOUNTED CASH FLOW MODEL

Geothermal cost models typically report LCOE for direct comparison with other renewable energy sources. However, LCOE summarizes the total lifetime costs of a power plant scaled by the total power generation from start-up to plant decommissioning. It is not well-suited for communicating projected net gains or losses under different plant concepts or flexible design scenarios, which are the focus of the present analysis. Instead, we rely on Net Present Value (NPV), a simple measure of project worth that accounts for the time value of money by applying a single interest rate, the discount rate, for both borrowing and deposits (de Neufville & Scholtes, 2011, pp. 195–215). Here, "present value" refers to a 2020 cost basis. For power generation over a 30-year lifespan –the default for geothermal models like GETEM (Entingh et al., 2006)– this basis takes the model out to 2050, a typical benchmark year for future projections.

5.1 Net Present Value

Following the outline for geothermal cost modeling from previous work (e.g., Augustine, 2009; Beckers et al., 2013; Tester et al., 2006), we consider revenue (R), operating & maintenance costs (OPEX or OM), and capital expenditures (CAPEX or C) as the primary components defining annual cash flow:

$$NPV = \sum_{t=1}^{T} D_t \cdot (R_t - C_t - OM_t). \tag{1}$$

Revenue and expenses are treated on an annual basis, meaning shorter-term fluctuations like price and production seasonality are not explicitly modeled. D_t in Equation (1) defines the time-based conversion factor between cash flow for a specific year (t) and discounted cash flow for the basis year.

5.2 Revenue

Annual revenue calculations rely on an estimate of power production within a year (W) and the power purchase agreement pricing (p_{PPA}) for that electricity (Entingh et al., 2006):

$$R = W p_{\mathrm{PPA}} = (\mathrm{b}_e \dot{m})\, p_{\mathrm{PPA}}, \tag{2}$$

where $\dot{m}$ is the mass flow rate of produced subsurface brine. We use the same empirical relationship with brine temperature (°C) for defining brine effectiveness (b_e) as is implemented for the GETEM model (Entingh et al., 2006, p. 62).

5.3 CAPEX

We decompose capital expenses into five sub-components associated with exploration, drilling, reservoir stimulation, fluid distribution, and power-plant costs.

$$C_t = \left[C_{\mathrm{expl}} + C_{\mathrm{dc}} + C_{\mathrm{stim}} + C_{\mathrm{dist}} + C_{\mathrm{pp}}\right]_t. \tag{3}$$

5.3.1 Exploration Capital Expenses

Exploration costs use the 2012 GETEM model estimate, which assumes slim hole (3–6″ diameter) drilling for exploration at a 60% discounted cost compared to standard-sized (≥ 8.5″ diameter) geothermal wells (EERE, 2012):

$$C_{\mathrm{expl}} = PPI \cdot [1.12\ (\$1\mathrm{M} + 0.6\ C_{\mathrm{dc}})]. \tag{4}$$

The constant $1 million term accounts for pre-drilling costs, including fieldwork, geophysical surveys of field structure, and interpretation of results (EERE, 2012). An additional 12% applied to the estimate covers technical and office support (EERE, 2012). Total exploration costs are converted to a 2020 cost basis using the Producer Price Index (PPI) for electric power generation from the U.S. Bureau of Labor and Statistics (U.S. BLS, 2021b).

5.3.2 Drilling Capital Expenses

Geothermal drilling costs differ from traditional oil & gas wells due to differences in hole diameter, thermal and geochemical conditions, and the strength and abrasiveness of the target formations (Lowry, Finger, et al., 2017). For our model, we use an empirical cost curve from GEOPHIRES (Eq. 4, Beckers et al., 2013):

$$C_{\mathrm{dc}} = PPI \cdot [1.65 \times 10^{-5}\ \mathrm{MD}^{1.607}], \tag{5}$$

where C_{dc} is measured in \$M and MD refers to measured depth in meters.

Each power-plant module requires an injector-producer pair, so Equation (5) represents one-half of the drilling cost per module. Drilling costs are converted to a 2020 cost basis using the *PPI* for electric power generation (U.S. BLS, 2021b). Note that Equation (4) was derived for well depths of 1600–9000 m. The hypothetical wells in this analysis could extend slightly shallower than this range, so Equation (4) should be viewed as a minimum drilling estimate.

5.3.3 Stimulation Capital Expenses

EGS at Lightning Dock requires stimulation of the Horquilla reservoir to create fluid pathways for thermal extraction. We apply stimulation costs described in the recent GeoVision analysis (Lowry, Finger, et al., 2017):

$$C_{\mathrm{stim}} = \$1\ 250\ 000\ n_{\mathrm{inj}}, \tag{6}$$

where n_{inj} describes the number of injection wells. As this represents a recent ballpark estimate, no cost basis conversion was applied in the model. Equation (6) may be high since it includes the cost of water, which should be available as wastewater from adjacent hydrothermal operations. The model only invokes stimulation costs for the injection well in each injector-producer pair.

5.3.4 Distribution Capital Expenses

Fluid-distribution costs include the entire surface piping system between the wells and power-plant modules. We use the GEOPHIRES estimate (Beckers et al., 2013):

$$C_{\mathrm{dist}} = PPI \cdot [\$50\ 000\ q_{\mathrm{in}}], \tag{7}$$

where q_{in} is the heat input from the produced brine, and PPI is the cost basis conversion factor. To estimate q_{in} from the production brine temperature, we apply the utilization efficiency relationship for a sub-critical binary-cycle plant from Beckers (Eq. 4.25, 2016).

Under the scenario where modular power-plant units are prefabricated and provided by a vendor, fluid distribution may be included in the installation fees. Distribution capital expenditures would be subsumed by power-plant costs (C_{pp}) and C_{dist} would reduce to zero. However, we were unable to confirm this fee structure and chose to include C_{dist} as described in Equation (7).

5.3.5 Power Plant Capital Expenses

Power-plant costs for a modular installation remain a source of significant uncertainty for our cost model. Schochet & Cunniff (2001) predicted fluid temperatures of 137–160 °C for the Lightning Dock EGS reservoir, which equates to \$2230–\$2415 per kW using the GEOPHIRES temperature-variable cost estimate for a binary-cycle power plant converted to a 2020 basis (Beckers et al., 2013).

If power-plant capacity is modularized with prefabricated units, economies of scale should reduce the cost of construction and installation. Without confirmation from a commercial module vendor, we chose a round-number estimate accounting for a modularity discount (Equation (8)). This estimate should be replaced by more accurate numbers when those values become available:

$$C_{\mathrm{pp}} = \$2000\ W, \tag{8}$$

where W is the electricity output of the plant in kW. We assume pump costs are included in this expense.

5.4 OPEX

Operations and maintenance expenses subdivide into costs for the power plant, wells, and water management:

$$OM_t = \left[OM_{\mathrm{pp}} + OM_{\mathrm{well}} + OM_{\mathrm{water}}\right]_t. \tag{9}$$

5.4.1 Power Plant Operating Expenses

We use a relationship based on labor costs (C_{labor}) and plant capital expenses (C_{pp}) from GETEM and GEOPHIRES (Eq. 9, Beckers et al., 2013) for power-plant O&M costs:

$$OM_{\mathrm{pp}} = 0.75\ C_{\mathrm{labor}} + 0.015\ C_{\mathrm{pp}}. \tag{10}$$

We applied the labor cost by plant capacity formula defined for GEOPHIRES (Eq. 10, Beckers et al., 2013) and converted it to a 2020 cost basis using the Employment Cost Index for total compensation for private industry utilities workers (U.S. BLS, 2021a). Due to lack of benchmark data, we chose not to scale this value for a modular installation compared to the traditional power plants from which this estimate was derived.

5.4.2 Well Operating Expenses

We included O&M costs per geothermal well based on labor (C_{labor}) and drilling (C_{dc}) expenses using the relationship described for GEOPHIRES (Eq. 12, Beckers et al., 2013):

$$OM_{\text{well}} = 0.25\ C_{\text{labor}} + 0.01\ C_{\text{dc}}. \tag{11}$$

We multiply Equation (11) by 2 for each module to represent costs for an injector-producer pair.

5.4.3 Water Operating Expenses

Water expenses refer to make-up water that replaces subsurface losses to the reservoir. We use the relationship built into the GETEM model (EERE, 2012):

$$OM_{\text{water}} = PPI \cdot [\$300\ V_{\text{loss}}], \tag{12}$$

where V_{loss} is water loss in units of acre-feet and PPI converts this estimate to a 2020 cost basis. Note that this operating cost could be alleviated by relying entirely on wastewater from Lightning Dock hydrothermal operations. We chose to include it in our cost model for a more conservative cost estimate.

5.5 Rate Calculations

We consider four rates when performing the NPV calculation: discount rate, learning rate, thermal drawdown rate, and capacity factor degradation rate.

5.5.1 Discount Rate

The discount rate defines the time value of money and is held constant throughout the modeled period. Equation (13) describes how discount rate re-scales cash flow to a present "discounted" value for the basis year (de Neufville & Scholtes, 2011, p. 199):

$$DCF = \frac{CF}{(1+r)^t}, \tag{13}$$

where DCF is discounted cash flow, CF is the cash flow for a specific year, r is the discount rate, and t represents the number of years between the modeled year and the basis year. D_t is equivalent to $1/(1+r)^t$ in Equation (1).

5.5.2 Learning Rate

We apply learning to EGS well-drilling costs for the area as a result of accumulated operator knowledge and experience, using the following relationship (de Neufville & Scholtes, 2011, p. 213):

$$U_i = U_1 i^{\beta}, \tag{14}$$

where U_1 and U_i are the costs to drill the first and i^{th} wells, respectively, i is the total well count, and β is the learning elasticity or slope of the empirically-derived learning rate ($\log i$, $\log U_i/U_1$) curve.

5.5.3 Thermal Drawdown Rate

The thermal drawdown rate defines the progressive cooling of the stimulated reservoir over time. We track this effect by reducing the produced brine temperature with each year of continued production similar to the GETEM model (Entingh et al., 2006):

$$T_n = T_0\,(1-d)^n, \tag{15}$$

where T_0 is the original reservoir temperature, T_n is the temperature of produced fluids at year n since drilling and stimulation activities last took place, and d is the thermal drawdown rate.

5.5.4 Capacity Factor Degradation Rate

Some geothermal techno-economic models account for natural long-term production degradation of plant performance over the lifetime of the asset (e.g., Gifford & Grace, 2013). We included capacity factor degradation by applying the following relationship in our model:

$$C_n = C_0(1-a)^n, \tag{16}$$

where C_0 is the original power-plant capacity factor, C_n is the capacity factor at year n since the power plant commenced operations, and a is the degradation factor.

5.6 Model Parameters

The following tables list the parameter values we selected for our cost model with sources indicated where appropriate. These values represent the Lightning Dock area and geothermal system components to the best of the authors' knowledge.

Table 1: Parameters related to resource recovery in the cost model

Parameter	Symbol	Value	Source
Ambient surface temperature	T_a	15.8°C	(Dahal et al., 2012)
Average geothermal gradient	∇T	100 K/km	(Crowell & Crowell, 2014)
Initial average reservoir temperature	T_0	149°C	(Schochet & Cunniff, 2001)
Cooling in the production well	ΔT_w	7.5%	(Lowry, Finger, et al., 2017)
Flow rate per production well	$\dot{m}$	35 kg/s	(Climeon, 2021)
Thermal drawdown	d	0.5%	(Entingh et al., 2006)
Water loss	ΔV_w	2%	(Blair et al., 2018)

Table 2: Parameters related to field and plant operations

Parameter	Symbol	Value	Source
Plant capacity factor	f_c	95%	(Glassley, 2015, p. 309)
Plant degradation factor	a	0.5%	(Augustine et al., 2019)
Well redevelopment factor	f_{rd}	85%	(K. Prestidge, pers. comm., Apr 29, 2021)

Table 3: Parameters related to economic factors and flexibility

Parameter	Symbol	Value	Source
Discount rate	r	7%	(EERE, 2012)
Learning elasticity	β	-0.1269	(Fig. 13, Lukawski et al., 2014)
Price premium for PPA	P_{PPA}	50%	(PNM, 2014)
Price trigger for flexibility	θ_{flex}	25%	N/A, for flexible design
Expansion factor	ϕ_{exp}	25%	N/A, for flexible design
Reduction factor	ϕ_{red}	25%	N/A, for flexible design

5.7 Electricity Prices

We used the industrial electricity price forecast for the Mountain region (including New Mexico) provided by the EIA in their Short Term Energy Outlook (STEO) projections to 2023 as a proxy for wholesale prices in the cost model (EIA, 2021a). We then ran the Forecast Tool in Excel to push the 1990–2023 time series to 2050 with 95% confidence bounds based on the built-in ETS (Exponential Triple Smoothing) algorithm (Microsoft, 2021). For the cost model, we directly sample a price from the forecast curve for any year when capacity increases, then multiply by the PPA price premium value listed in Table 3. This simulates amending the PPA with a local utility whenever additional capacity is available for power sales. Electricity pricing is held flat compared to the previous year when no capacity change occurs in accordance with an in-place PPA.

6. PARAMETER SENSITIVITY TESTING

We incorporate parameter uncertainty in our economic model by replacing static values with distributions for model variables. However, all variables in the model have some underlying uncertainty, and defining distributions for every parameter would add significant complexity to the model. We therefore used sensitivity testing to determine an importance ranking of multiple sources of uncertainty.

Characterizing the full realistic range of parameter values and the underlying forces controlling those values requires a deep understanding of the scientific, engineering, and socio-technical elements influencing the system. For geothermal, subsurface-characterization uncertainties play an important role, but so do the uncertainties tied to public policy and market dynamics. We limit our focus to the list below as a fit-for-purpose demonstration of the methodology. Additional variables can and should be considered, including externalities as appropriate ways to characterize them come to light.

- Reservoir Temperature: Schochet & Cunniff (2001) noted the Horquilla formation temperature range is likely 280–320°F.
- Geothermal Gradient: Wells TG12-7 and TG56-14, located approximately 1 km and 4 km away from the center of the hydrothermal plume at Lightning Dock, have reported gradients of 80–120 K/km (Cunniff & Bowers, 2003).
- Ambient Temperature: A range of model scenarios for New Mexico predicted up to 4.2 °C increase in statewide ambient temperatures by 2050, up from the present baseline of 1.1 °C over pre-industrial levels (Frankson et al., 2019).

- Thermal Drawdown Rate: The GeoVision report uses 0.5–0.6%/year for modeling thermal drawdown rate (Augustine et al., 2019), although prior published models applied values of up to 4%/year (Tester & Herzog, 1990).
- Drilling Costs: Multiple scenario-based drilling-cost curves derived in association with the GeoVision study (Fig. 1, Lowry, Foris, et al., 2017) predict a drilling cost range of $1–$3 million for the estimated target reservoir depths.
- Carbon Taxation: A study from Columbia University on carbon tax scenarios predicts a step-up in electricity prices that remain steady-state over the modeled decade after that (Larson et al., 2018). The price increased by 28% for the highest tax case analyzed compared to the base case of no carbon tax.
- National Electrification: The Electrification Futures Study forecasts swings in electricity prices based on various widespread electrification scenarios (Murphy et al., 2021). Considering only High Future Electrification cases, modeled electricity prices in 2050 vary from 23% lower than the base case for the Low Renewable Technology Costs case to 50% greater for the Constant Renewable Technology Costs case (NREL, 2021a).

The tornado diagram in Figure 4 illustrates model sensitivity results relative to a baseline static model where five modules are installed at the project start, power pricing varies annually (i.e., no long-term PPA), and the model parameterization matches Table 1–Table 3. Variability in thermal drawdown rate acts as a strong control on model performance, followed by modest influences from reservoir temperature, drilling costs, future electrification price changes, and geothermal gradient. Uncertainty in the ambient surface temperature and price impact of a carbon tax have an order of magnitude less impact on project NPV than other uncertainties.

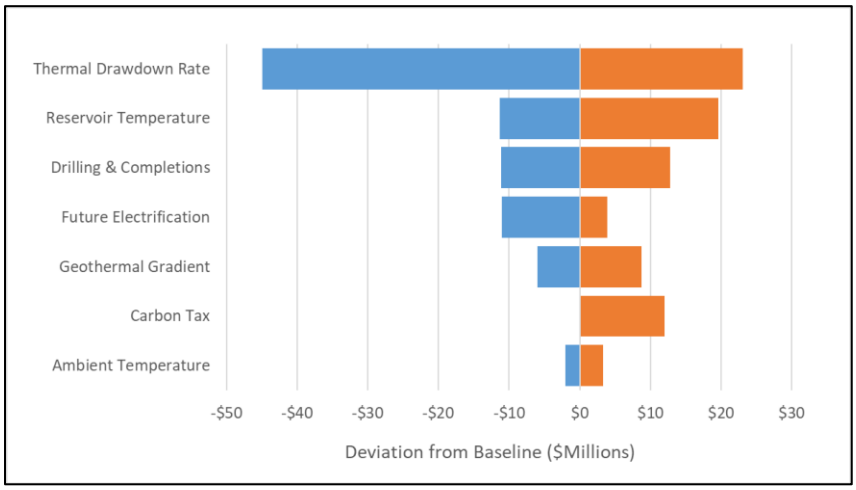

Figure 4: Tornado diagram for different model uncertainties. Horizontal axis measures deviation from a baseline static model.

7. PARAMETER DISTRIBUTIONS

Having established the critical sources of uncertainty, we defined probability density functions (PDFs) to the key model parameters for use as part of a stochastic NPV assessment. The thermal drawdown rate PDF uses a beta distribution such that its P_{50} value aligns with 0.5%, 4.0% represents the $P_{97.5}$ case, and a superimposed linear trend from P_{95}–P_{100} caps the rate at 5.6% (Figure 5A). We model reservoir temperature (Figure 5B) and geothermal gradient (Figure 6A) as normal distributions using the range bounds tested in Section 6 to define the P_{05} and P_{95} percentiles. Drilling cost is modeled as a triangular distribution (Figure 6B), with a peak probability for the static model estimate and extrema values approximated from the GeoVision study (Fig. 1, Lowry, Foris, et al., 2017).

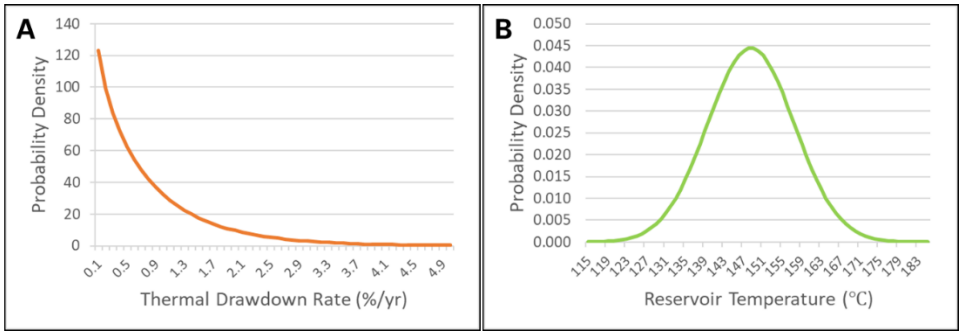

Figure 5: PDFs for A. thermal drawdown rate and B. reservoir temperature

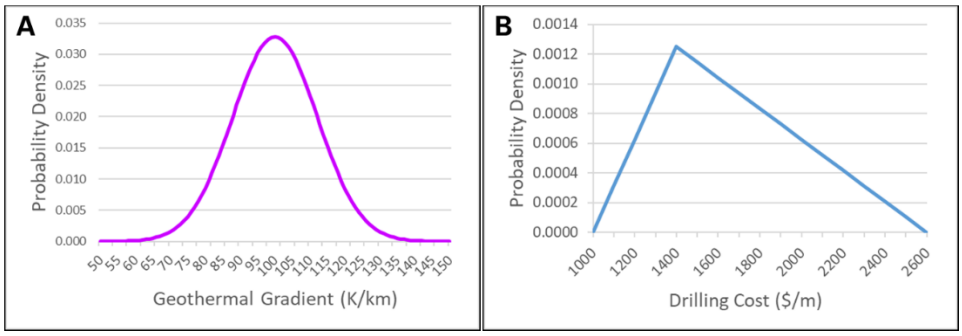

Figure 6: PDFs for A. geothermal gradient and B. drilling cost.

We also added uncertainty to the electricity-price curve in two ways. First, a step-change occurs on a randomly-selected year between 2020–2050 to capture a sudden market response to energy-transition events. The magnitude of the step is determined from a uniform distribution built using the spread of outcomes from the Electrification Futures Study (Murphy et al., 2021). An example of how this randomly-timed, randomly-sampled step-change affects the electricity price curve is shown as the dotted curve in Figure 7A. Second, we added volatility by introducing randomly-sampled Gaussian offsets using the 95% confidence bounds for each forecast year on the price curve. This method produces a unique price projection for each simulation of the model. We show a single realization of the randomly-perturbed forecast as the dotted curve in Figure 7B.

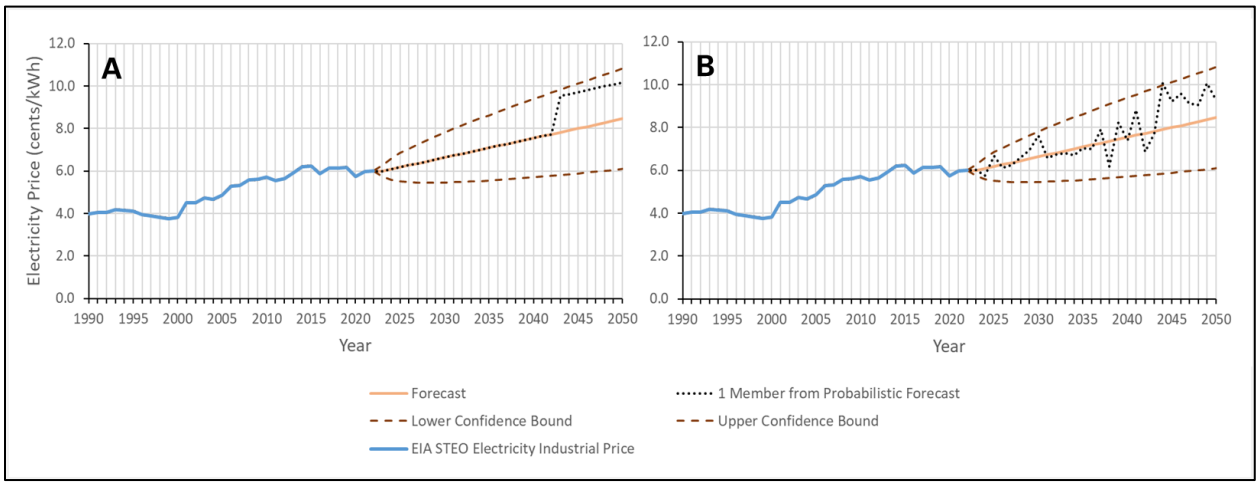

Figure 7: Price of electricity from the EIA STEO (blue), forecast out to 2050 (orange) with 95% confidence intervals (brown). Uncertainty is added by superimposing A. a randomly-defined step change in pricing and B. annual Gaussian volatility to produce a unique price curve for each simulated model run (dotted black).

8. OPTIMIZED INSTALLATION SCHEDULE

The installation of a Lightning Dock EGS expansion could take place over a variety of different schedules due to system modularity. Rather than assume the greatest profit would be achieved by front-end loading the power-plant capital expenditures, we optimized the deployment schedule by exploring different permutations of installation timing for five binary-cycle modules over the first five years. We also compared modeling with either a fixed capacity (5 MW) or with a fixed flow rate (35 kg/s) since both options are supported by a power generation model formulation based on brine effectiveness (Entingh & Mines, 2006, p. C–8). Results were calculated using the expected value of NPV (ENPV) from 5000 scenarios run using the probabilistic parameter representations described in Section 7.

The fixed-capacity model results in project losses of ≈ $25–30 million for all tested installation options (Figure 8). By contrast, the fixed flow-rate model remains closer to –$8–15 million ENPV. The best-performing forecasts include at least one module installation in the fifth year. The second-best group of forecasts deploys all modules within the first three years. An investment in all five modules at the project start produces the worst ENPV estimate. Although several installation schedules show similar economics, we observe a maximum when two modules are installed on year 1, two more on year 2, and a fifth on year 5 (red arrow, Figure 8). Based on these results, all further analysis applies this installation schedule and assumes a fixed flow rate per production well, as noted in Table 1.

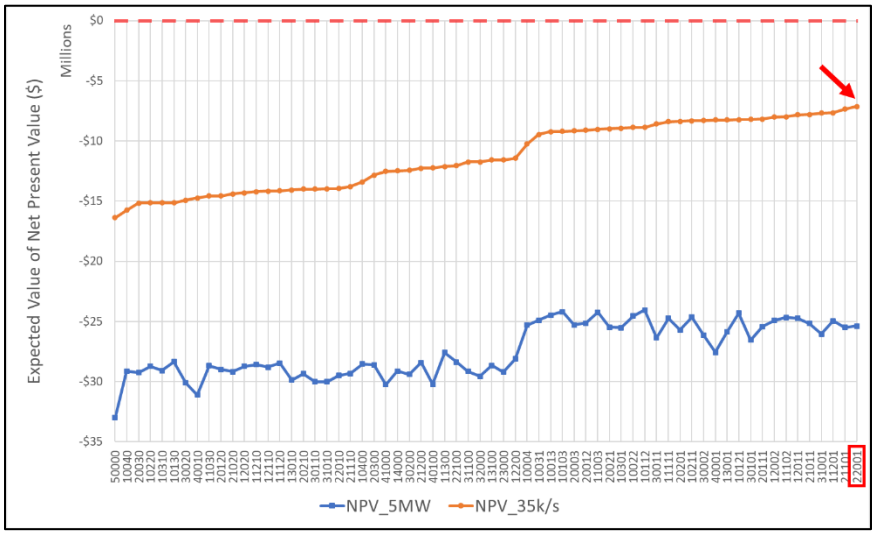

Figure 8: Probabilistic cost model comparison between fixed capacity (blue) and fixed flow rate (orange) calculation methods, plotted against installation schedule. Sequence labels on the horizontal axis describe the number of modules installed per year, such that digit d_i in schedule $d_1d_2d_3d_4d_5$ defines that $d_i \in \{0, 1, 2, 3, 4, 5\}$ modules are installed in year i. A total of $\sum_{i=1}^{5} d_i = 5$ modules are installed in each of the schedules. The axis is sorted on fixed flow rate (35 kg/s) model ENPV. The red arrow and box identify the optimal scenario used in this study.

9. BASE CASE COMPARISON

Using the parameterization described in Table 1–Table 3 and the installation schedule defined in Section 8, the static model predicts an EGS NPV of –$2.9 million. This value serves as a benchmark for the probabilistic models described throughout the rest of this paper.

The Base Case probabilistic model mimics the static model in form but uses randomly-sampled values from the PDFs in Section 7 when performing model calculations. We generated a Monte Carlo ensemble of 5000 simulated realizations to derive the set of summary statistics and the histogram shown in Figure 9.

Base Case Statistics	
ENPV	-7.6
STD(NPV)	20.8
SKEW(NPV)	0.1
KURT(NPV)	-0.2
P05 NPV	-42.5
P50 NPV	-7.2
P95 NPV	26.0
% Difference from NPV_s	158%

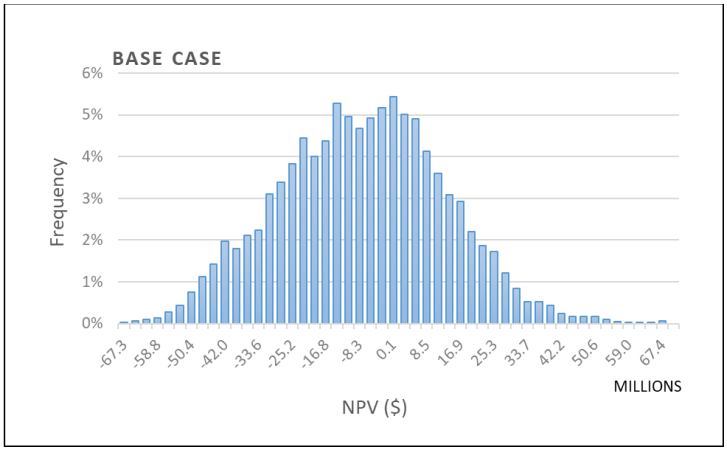

Figure 9: (Left) Base case probabilistic model statistics for 5000 model realizations. NPV is reported in $ millions. NPV_s refers to the static model NPV. (Right) Histogram of modeled NPV from the 5000 realizations.

At –$7.6 million ENPV, the Base Case model predicts ≈ 160% lower project value than predicted for the static model. This result illustrates how probabilistic approaches can significantly differ from deterministic models that use most-likely or average values. Skewed system performance occurs even when variable distributions are balanced, making deterministic results unrealistic and unreliable measures for decision-making (de Neufville & Scholtes, 2011, pp. 48–49). Here, an unanticipated high-side (e.g., P_{95} = $26 million) does exist, but the influence of the low-side (e.g., P_{05} = –$42.5 million) dominates overall. Cumulatively, over 60% of the realizations end in a net loss for the project. Furthermore, at 3× both the median and ENPV, the standard deviation of NPV indicates this solution is not particularly robust. Low skewness (0.1) and slightly negative kurtosis (-0.2) capture the symmetry and thick-tailed aspects of the NPV distribution.

10. STRATEGY TESTING WITH DECISION RULES

Given the negative ENPV, high likelihood of project financial loss, and no strategy for mitigating risk, a responsible project manager should conceivably reject the Base Case project plan. However, this probabilistic model maintains a fixed design regardless of the emergent conditions that would likely trigger changes during real-life operations. Flexible design provides options that can be exercised

in the future if it benefits system stakeholders (de Neufville & Scholtes, 2011, p. 134). We mimic this flexibility in our model by implementing logical decision rules —essentially IF…THEN statements— which govern how the model behaves based on past observations. Decision rules may act independently or be chained together to reveal otherwise hidden financial value. The following scenarios extend the Base Case model with decision rules that define mitigation strategies for the EGS expansion project.

10.1 Redevelopment Only

Sensitivity testing revealed that the thermal-drawdown rate is the most critical uncertainty governing cost-model performance (Figure 4). Over time, cooling of the reservoir by injected fluids results in declining input temperatures to the binary cycle plant and hence lower electricity generation. If the latter drops below a certain level, well redrilling or restimulation must occur. The GETEM model implements a full field redrill campaign based on a threshold reservoir temperature (Entingh et al., 2006), which we emulate with our Redevelopment Only strategy. Specifically, we implement the GETEM threshold and commit to redeveloping (redrill with stimulation) when production temperatures decline too far. Figure 10 shows the results for a Monte Carlo simulation with 5000 runs of this model.

Redevelopment Only Statistics	
ENPV	-2.4
STD(NPV)	17.8
SKEW(NPV)	-0.1
KURT(NPV)	0.9
P05 NPV	-30.6
P50 NPV	-2.6
P95 NPV	27.0
% Difference from NPV_S	-18%

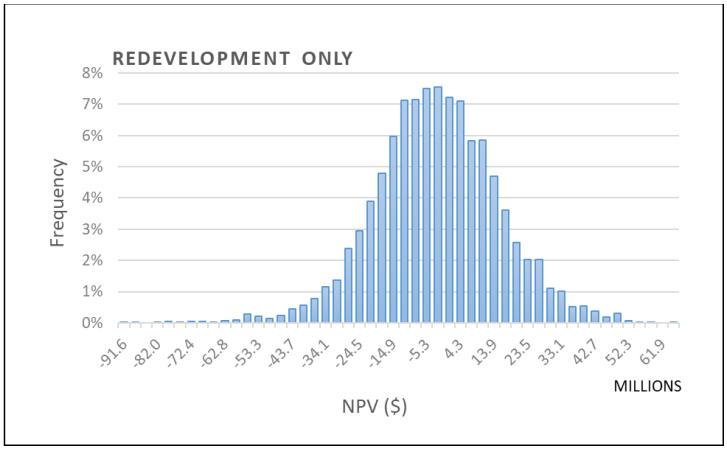

Figure 10: (Left) Redevelopment Only strategy statistics for 5000 model realizations. NPV is reported in $ millions. NPVs refers to the static model NPV. (Right) Histogram of modeled NPV from the 5000 realizations.

Adding the well redevelopment decision rule improves project ENPV by $5.2 million over the Base Case; however, it remains negative at −$2.4 million, 18% below the static model NPV. The distribution skewness stays low, but kurtosis (0.9) increases due to thinner tails and a more pronounced central peak. Value-at-risk (P_{05} value of −$30.6 million) decreases by over $10 million relative to the Base Case. This demonstrates the improvement potential in overall production and power sales by managing reservoir conditions. As a brief caveat: the idea of periodic redevelopment for a geothermal field is not novel. Nevertheless, the analysis above illustrates why this design option should be included in geothermal modeling and operations to help mitigate the risk of high thermal-drawdown rates.

10.2 Restimulation Only

A re-drilling campaign is an aggressive response to thermal decline and comes with the financial disincentive of high geothermal-drilling costs. If we instead assume restimulation will rejuvenate accessible reservoir thermal conditions by creating new fluid pathways, we can model a more cost-effective strategy of only restimulating in response to thermal decline. Figure 11 presents the results of the simulation under this decision rule.

Restimulation Only Statistics	
ENPV	0.1
STD(NPV)	15.1
SKEW(NPV)	0.5
KURT(NPV)	0.5
P05 NPV	-22.0
P50 NPV	-1.4
P95 NPV	26.6
% Difference from NPV_S	-103%

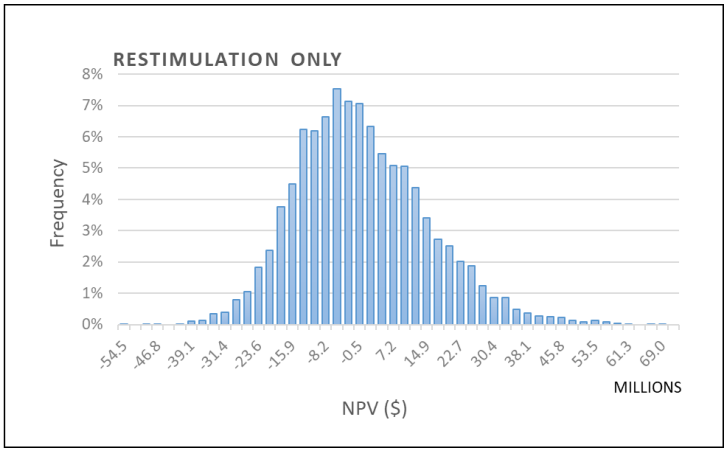

Figure 11: (Left) Restimulation Only strategy statistics for 5000 model realizations. NPV is reported in $ millions. NPVs refers to the static model NPV. (Right) Histogram of modeled NPV from the 5000 realizations.

A Restimulation Only strategy brings ENPV into break-even territory at $0.1 million. Positive skewness (0.5) highlights the longer right tail that defines positive outcomes in the distribution. However, the value-at-risk remains undesirable at P_{05} = –$22 million. For the EGS expansion proposal to gain traction with an operator, additional strategies must be pursued to make the economics more attractive.

10.3 Restimulation & Growth

The Restimulation & Growth strategy adds a decision rule for increasing aggregate nameplate capacity. When electricity prices rise by an amount larger than a monitored threshold (25%, see Table 3), the operator responds by installing new power-plant modules to capitalize on the increased prices and inferred demand. We also continue to apply the restimulation rule to maintain the temperature of produced brine. Simulation results for this strategy are provided in Figure 12.

Restimulate & Growth Statistics	
ENPV	6.3
STD(NPV)	17.9
SKEW(NPV)	0.5
KURT(NPV)	0.4
P05 NPV	-20.4
P50 NPV	4.7
P95 NPV	38.2
% Difference from NPV_S	-312%

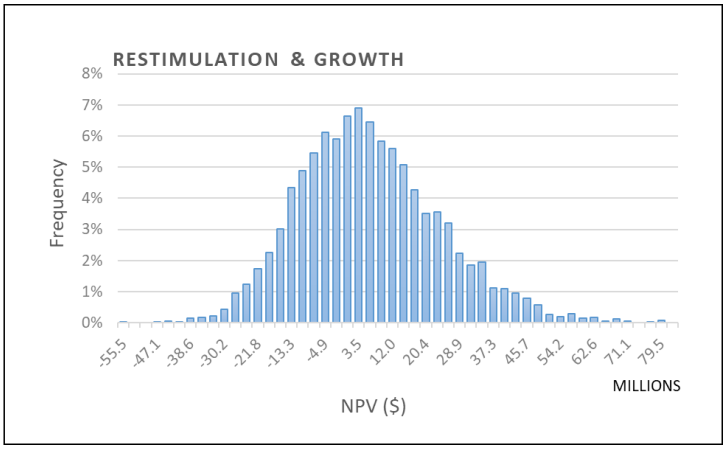

Figure 12: (Left) Restimulation & Growth strategy statistics for 5000 model realizations. NPV is reported in $ millions. NPVs refers to the static model NPV. (Right) Histogram of modeled NPV from the 5000 realizations.

In our model, we assume that the power purchase agreement (PPA) with a utility company gets successfully renegotiated when new modules go online such that additional power generation immediately feeds into revenue. The model predicts an ENPV of $6.3 million, the first strategy to achieve a moderate expected profit. Like the Restimulation Only strategy, kurtosis is positive, and the distribution is right-skewed. The P_{95} prediction exceeds $38 million. Negative financial outcomes occur just under 40% of the time, including –$20 million for the P_{05} value-at-risk. This strategy captures value but does not remove risk.

10.4 Full Flexibility

In our final tested strategy, Full Flexibility, we add a decision rule to Restimulation & Growth that reduces aggregate plant capacity if electricity prices drop by a threshold amount (25%, see Table 3). Power-plant modules are proactively decommissioned to reduce electricity production and operating expenses. Although a PPA would protect prices, we assume that a significant shift in the electricity market would eventually lead to renegotiations with the partner utility company, and the operating company could respond with field-capacity adjustments. If adjustments occur and the PPA price drops with the market, the results match the Restimulation Only scenario with an ENPV ≅ $0 (not shown). Figure 13 illustrates the results for the Full Flexibility strategy where PPA pricing remains unchanged as capacity reductions are triggered, i.e., in an assumed compromise between the operator and utility company.

Full Flexibility Statistics	
ENPV	3.1
STD(NPV)	16.8
SKEW(NPV)	0.4
KURT(NPV)	0.3
P05 NPV	-22.5
P50 NPV	1.8
P95 NPV	33.3
% Difference from NPV_S	-205%

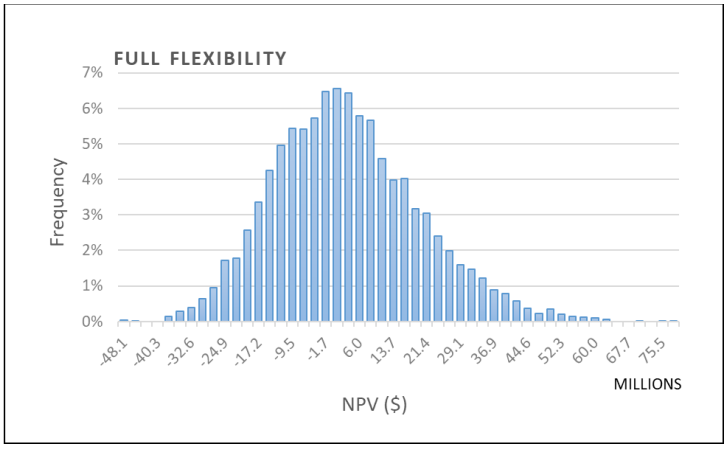

Figure 13: (Left) Restimulation, Growth, and Reduction (Full Flexibility) strategy statistics for 5000 model realizations. NPV is reported in $ millions. NPVs refers to the static model NPV. (Right) Histogram of modeled NPV from 5000 realizations.

The Full Flexibility strategy financially underperforms the Restimulation & Growth strategy with an ENPV of $3.1 million. We observe a comparatively tighter distribution as evidenced by the smaller standard deviation. Positive skewness (0.4) highlights the continued presence of an extended right tail in the results. However, median ENPV dropped by nearly $3 million compared to Restimulation & Growth, and narrowing is most notable on the high-side with a $5 million drop in P_{95} value-at-gain.

11. STRATEGY COMPARISON

Figure 14 shows the target curves for the different probabilistic models. The Base Case model (orange) is dominated by all other models on the low side and merges with the Redevelopment Only (gray) and Restimulation Only (blue) strategies on the high side. Full Flexibility (green) separates from the Restimulation Only curve on the low side and dominates the others across mid-probability ranges; however, it is dominated by Restimulation & Growth (yellow) across nearly all percentiles. Nevertheless, the Restimulation & Growth curve has one of the smallest slopes, indicating a high standard deviation and low relative confidence among the tested strategies. Depending on the risk tolerance of an operator, either Restimulation & Growth could be the selected operational strategy due to its upside potential, or the Full Flexibility strategy would be preferred because of its slightly tighter range of outcomes.

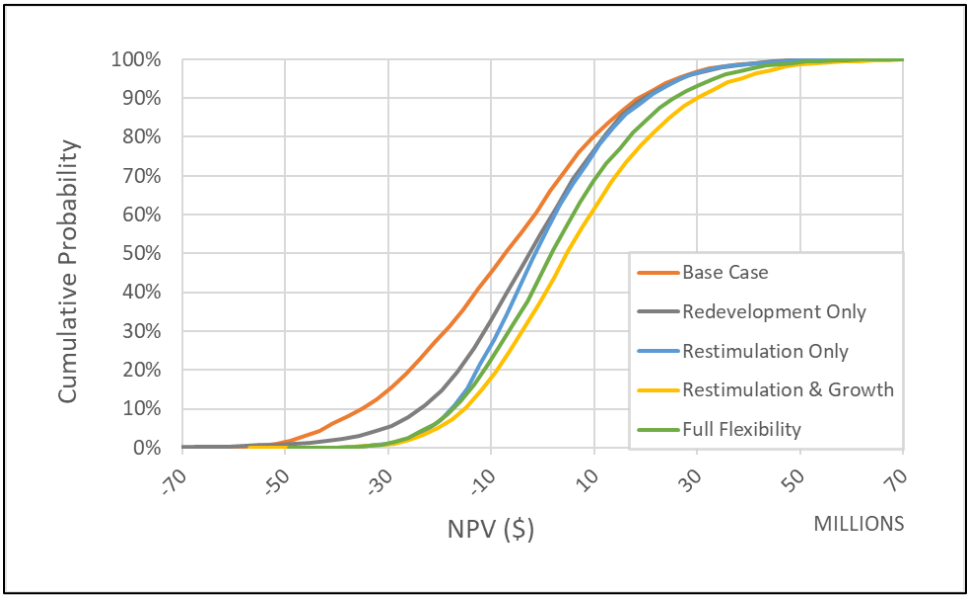

Figure 14: Cumulative distribution functions (target curves) for all probabilistic cases described in Sections 9–10. Each curve summarizes model results based on a 5000-run Monte Carlo simulation.

12. DISCUSSION

In this case study, we covered an economic-modeling workflow to test the feasibility of an EGS expansion of the Lightning Dock power plant. Among the uncertainties tested for model sensitivity, thermal-drawdown rate and reservoir temperature demonstrate the most significant influence on project profitability (Figure 4). Drilling costs play an important role, but sensitivities indicate that reducing the uncertainty of subsurface conditions is paramount to defining geothermal-project economics. Surprisingly, surface conditions affect NPV to a much lesser extent. We certainly expect the efficiency of air-cooled binary-cycle plants in semi-arid New Mexico to decline as local conditions increase in average temperature. Replacing the brine efficiency calculation (Equation (2)) with a more rigorous binary-cycle plant simulator in the future would help validate the model insensitivity to ambient conditions expressed in Figure 4.

Project losses associated with static operations over the life of the project could not be fully mitigated by responding to thermal decline alone in our model. Modular power-plant technology supports rapid expansion or incremental reduction of aggregate capacity, and exercising this flexibility moved modeled ENPV into positive territory. However, a strategy that incorporates capacity growth and reductions (Full Flexibility) underperformed one that simply installs new modules with significant electricity price changes (Restimulation & Growth). Both strategies rely on pre-set parameters that determine the size of capacity expansion or reduction, listed in Table 3. We tested the influence of these values by conducting a sensitivity test illustrated in Figure 15.

When the expansion factor is reduced to zero, the Restimulation & Growth (gray) and Full Flexibility (yellow) models both consistently predict ENPV ≅ $0 across all reduction factor values. Resetting the expansion factor to its default value ($\phi_{\mathrm{exp}} = 0.25$) shifts Restimulation & Growth (blue) to a new ENPV level of ≈ $6 million, but Full Flexibility (orange) demonstrates step-like behavior of decreasing project value with increasing reduction factor. We interpret this trend as a system response to the insulating effect introduced by the PPA, such that declining prices do not trickle down to annual power purchases. In fact, removing capacity works against the interests of the operator because it reduces a stream of revenue otherwise maintained irrespective of the electricity market, and that cut in income outweighs the OPEX cost savings. Down-steps in the Full Flexibility curve depict value lost from removing additional power-plant modules during the lifetime of the field, making the optimal value for the reduction factor effectively zero (Figure 15).

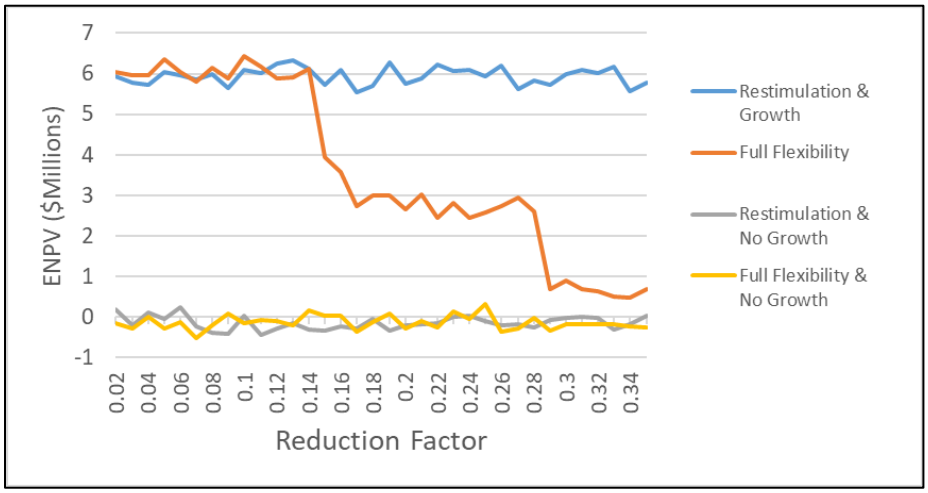

Figure 15: Sensitivity testing of the field expansion and reduction factors on ENPV when applying two operational strategies. The blue and orange lines illustrate results when the field expansion factor is assigned the default value ($\phi_{exp} = 0.25$) and the reduction factor (ϕ_{red}) is varied from 0.02 to 0.03 at an increment of 0.01. The gray and yellow lines track results when $\phi_{exp} = 0$ and no module additions occur during the simulated period.

Although we strived to accurately characterize the value ranges and select appropriate PDFs for all non-deterministic parameters in our model, a more thorough analysis would be prudent future work for this case study. Capturing realistic variation in the wholesale electricity market presents an even greater challenge. We propose integrating a more sophisticated market model to generate electricity price curves for each Monte Carlo realization. Additionally, a more comprehensive treatment of the system dynamics of Renewable Policy Standards (RPS), power purchase agreements, and the sensitivity of both to disruptive events like carbon taxation and national electrification would help test the trends described by our model. For example, the performance of the Restimulation & Growth model hinges on an assumption of immediate, guaranteed PPA updates securing the requisite power sales for newly-installed power-plant modules. New Mexico maintains an RPS with carve-outs appropriated for non-wind, non-solar renewables to diversify the energy mix (New Mexico Public Regulation Commission, 2021), so utilities would reasonably accept the offer for additional generated power over the near term. However, this policy may not hold for the full 30-year span considered by the model. We also recognize that the agility required to install new power-plant modules, including drilling an injector-producer pair, renegotiating a PPA, and beginning production within one year of a market trigger, may be somewhat optimistic.

Flexibility in this study focuses on geothermal power-plant modularity, but the concept is not unique to this application. A cost-modeling methodology enhanced by decision rules could generally apply to most engineering projects. However, design flexibility may not always be a desirable feature due to the complex interplay of multiple factors, including uncertainties internal and external to the system, economies of scale, learning effects, and the discount rate (de Neufville & Scholtes, 2011, pp. 209–215). Project decision-makers will benefit from models that test expected value forecasts for various design alternatives, with and without flexibility. This is particularly true for large-scale projects like industrial plants, where different engineering designs can result in tens of millions of dollars difference in project outcomes (Cardin et al., 2015). Since our small proof-of-concept EGS expansion project profited from considering design flexibility, we believe larger geothermal projects would as well.

13. CONCLUSIONS

This case study presented a spreadsheet-based techno-economic model for a modular EGS power plant expansion as an example of probabilistic cost-modeling paired with flexible design. The subsurface thermal resource, surface power generation system, and associated capital and operating expenses were assigned values for a deterministic case assessment. Enhancing the model with probability distributions and logical decision rules unlocked new potential for testing and optimizing field management strategies. Even with a negative Net Present Value (NPV) assessment, we found that the deterministic model overpredicted NPV due to its reliance on average or most-likely values rather than parameter distributions. Monte Carlo simulation instead predicted 2.6 × the magnitude of losses for our base scenario. Including well redevelopment or restimulation mitigates subsurface thermal drawdown and reduces the percentage of low-side model outcomes, but it does not make the project viable alone. Significant improvements to financial downside risk and upside capture are realized by flexibly increasing capacity and renegotiating power-purchase agreements (PPAs) based on a trigger for electricity price surges. Including flexibility to shut down power-plant modules when electricity prices plummet results in systematically lower NPV predictions. Further investigation of parameter sensitivities revealed an optimum when no power-plant modules are removed due to the PPA structure of revenue for power generators. We believe the applied methodology demonstrated here is a valuable template for future geothermal project modeling. Incorporating parameter uncertainties supports project scenario comparisons using expected value, target percentiles, and other practical measures. Design flexibilities offer even greater value by introducing optionality for capturing opportunities if they arise. Geothermal forecast models that integrate flexibilities simulate intelligent system management over the lifespan of a field, much to the benefit of project decision-makers. Furthermore, doing so is broadly achievable using home or business computational resources and the skills to operate widely-available spreadsheet software.

REFERENCES

Augustine, C. (2009). *Hydrothermal spallation drilling and advanced energy conversion technologies for engineered geothermal systems*. Massachusetts Institute of Technology.

Augustine, C., Ho, J., & Blair, N. (2019). *GeoVision Analysis Supporting Task Force Report: Electric Sector Potential to Penetration* (NREL/TP-6A20-71833). National Renewable Energy Lab. (NREL), Golden, CO (United States). https://doi.org/10.2172/1524768

Beckers, K. (2016). *Low-temperature geothermal energy: Systems modeling, reservoir simulation, and economic analysis* [Cornell University]. https://ecommons.cornell.edu/handle/1813/44328

Beckers, K., Lukawski, M., Reber, T., Anderson, B., Moore, M., & Tester, J. W. (2013). Introducing GEOPHIRES v1.0: Software Package for Estimating Levelized Cost of Electricity and/or Heat from Enhanced. *Geothermal Systems, Proceedings, Thirty-Eighth Workshop on Geothermal Reservoir Engineering*.

Beckers, K., & McCabe, K. (2018). GEOPHIRES V2.0 User Manual. In *UserManual.wiki*. https://usermanual.wiki/Document/GEOPHIRES20v2020User20Manual.1047423261/view

Beckers, K., & McCabe, K. (2019). GEOPHIRES v2.0: Updated geothermal techno-economic simulation tool. *Geothermal Energy*, *7*(1), 5. https://doi.org/10.1186/s40517-019-0119-6

Blair, N., DiOrio, N., Freeman, J., Gilman, P., Neises, T., & Wagner, M. (2018). *System Advisor Model (SAM) general description (version 2017.9. 5)* (Technical Report NREL/TP-6A20-70414). National Renewable Energy Lab.(NREL). doi:10.2172/1440404

Bonafin, J., Goodman, N., & Dickey, H. K. (2019). The Repowering of the Lightning Dock Geothermal Plant in New Mexico. *Geothermal Resources Council Bulletin*, *48*(6), 34–40.

Cardin, M., Ranjbar-Bourani, M., & De Neufville, R. (2015). Improving the lifecycle performance of engineering projects with flexible strategies: Example of on-shore LNG production design. *Systems Engineering*, *18*(3), 253–268.

Climeon. (2021). *The Climeon Heat Power System—How does it work?* The Climeon Heat Power System - How Does It Work? https://climeon.com/how-it-works/

Crowell, J., & Crowell, A. (2014). The History of Lightning Dock KGRA: Identifying a Blind Geothermal Resource. *GRC Transactions*, *38*, 8.

Cunniff, R. A., & Bowers, R. L. (2003). *Final Report Enhanced Geothermal Systems Technology Phase II Animas Valley, New Mexico* (DOE/ID/14203). Lightning Dock Geothermal INC. (US). https://doi.org/10.2172/820539

Dahal, S., McDonald, M. R., Bubach, B., & Crowell, A. M. (2012). Evaluation of geothermal potential of lightning dock KGRA, New Mexico. *Transactions of the Geothermal Resources Council*, *36*, 637–640.

de Neufville, R., & Scholtes, S. (2011). *Flexibility in engineering design*. MIT Press.

EERE. (2012). *GETEM -Geothermal Electricity Technology Evaluation Model*. U.S. Department of Energy. https://www.energy.gov/eere/geothermal/getem-manuals-and-revision-notes

EIA. (2021a). Short-Term Energy Outlook (STEO). In *US EIA - Short-Term Energy Outlook* (Issue October 6). https://www.eia.gov/outlooks/steo/

EIA. (2021b). Annual Energy Outlook 2021 (AEO2021). In *Annual Energy Outlook* (Vol. 2021) [Technical Report]. Government Printing Office. https://www.eia.gov/outlooks/aeo/

Engman, C. (2018). *Why low temperature geothermal heat power will become bigger that high temperature geothermal heat power?* Iceland Geothermal Conference, Reykjavik. https://www.slideshare.net/IcelandGeothermal/a3-why-low-temperature-geothermal-heat-power-will-become-bigger-that-high-temperature-geothermal-heat-power

Entingh, D., & Mines, G. (2006). GETEM Volume III-Detailed Technical Appendixes. *Geothermal Electricity Technology Evaluation Model (GETEM)*.

Entingh, D., Mines, G., Nix, G., Mansure, A., Bauer, S., Petty, S., & Livesay, B. (2006). GETEM Volume I–Technical Reference Manual. *Geothermal Electricity Technology Evaluation Model (GETEM)*.

Frankson, R., Kunkel, K., Stevens, L., & Easterling, D. (2019). New Mexico State Climate Summary. *NOAA Technical Report NESDIS*.

Gifford, J. S., & Grace, R. C. (2013). *CREST Cost of Renewable Energy Spreadsheet Tool: A Model for Developing Cost-Based Incentives in the United States; User Manual Version 4, August 2009 - March 2011 (Updated July 2013)* (NREL/SR-6A20-50374, 1010865; p. NREL/SR-6A20-50374, 1010865). National Renewable Energy Lab. https://doi.org/10.2172/1010865

Glassley, W. E. (2015). *Geothermal energy: Renewable energy and the environment* (2nd ed.). CRC press.

Larson, J., Mohan, S., Marsters, P., & Herndon, W. (2018). *Energy and Environmental Implications of a Carbon Tax in the United States*. Columbia University. https://energypolicy.columbia.edu/sites/default/files/pictures/CGEP_Energy_Environmental_Impacts_CarbonTax_FINAL.pdf

Lowry, T. S., Finger, J. T., Carrigan, C. R., Foris, A., Kennedy, M. B., Corbet, T. F., Doughty, C. A., Pye, S., & Sonnenthal, E. L. (2017). *GeoVision Analysis Supporting Task Force Report: Reservoir Maintenance and Development* (p. 80) [SAND2017-9977]. Sandia National Lab.

Lowry, T. S., Foris, A., Finger, J. T., Pye, S., & Blankenship, D. A. (2017). *Implications of drilling technology improvements on the availability of exploitable EGS resources*. Proceedings, 42nd Workshop on Geothermal Reservoir Engineering, Stanford University, Stanford, California.

Lukawski, M. Z., Anderson, B. J., Augustine, C., Capuano, L. E., Beckers, K., Livesay, B., & Tester, J. W. (2014). Cost analysis of oil, gas, and geothermal well drilling. *Journal of Petroleum Science and Engineering*, *118*, 1–14. https://doi.org/10.1016/j.petrol.2014.03.012

Microsoft. (2021). *FORECAST.ETS function*. https://support.microsoft.com/en-us/office/forecast-ets-function-15389b8b-677e-4fbd-bd95-21d464333f41

Murphy, C., Mai, T., Sun, Y., Jadun, P., Muratori, M., Nelson, B., & Jones, R. (2021). *Electrification futures study: Scenarios of power system evolution and infrastructure development for the united states*. National Renewable Energy Lab.

New Mexico Public Regulation Commission. (2021). *New Mexico Public Regulation Commission*. Utility - Renewable Energy. http://www.nmprc.state.nm.us/utilities/renewable-energy.html#gsc.tab=0

NREL. (2021a). *Cambium | Electrification Futures Study (EFS)*. https://cambium.nrel.gov/?project=fc00a185-f280-47d5-a610-2f892c296e51&mode=view&layout=Default

NREL. (2021b). *System Advisor Model (SAM)*. https://sam.nrel.gov/

Orcan Energy AG. (2021, March 12). *efficiency PACK 050.100: Product introduction*. https://www.youtube.com/watch?v=WiBPK_Lzeeo

PNM. (2014). *Public Service Company of New Mexico's Renewable Energy Portfolio Procurement Plan For 2015*. https://www.pnm.com/documents/396023/428013/Renewable_Plan_2015/8e4a68b7-5177-4e38-99c2-d3edf7f598c6

Prestidge, K. (2021, April 29). *Performance Drilling and Completions Engineer* [Personal communication].

Schochet, D. N., & Cunniff, R. A. (2001). *Development of a Plan to Implement Enhanced Geothermal Systems (EGS) in the Animas Valley, New Mexico—Final Report—07/26/2000—02/01/2001* (DOE/ID/13989). ORMAT International, Inc., Sparks, NV (US); Lightning Dock Geothermal, Inc., Las Cruces, NM (US). https://doi.org/10.2172/790039

Tester, J. W., Anderson, B. J., Batchelor, A., Blackwell, D., DiPippo, R., Drake, E., Garnish, J., Livesay, B., Moore, M., & Nichols, K. (2006). The future of geothermal energy. *Massachusetts Institute of Technology*, *358*.

Tester, J. W., & Herzog, H. J. (1990). *Economic predictions for heat mining: A review and analysis of hot dry rock (HDR) geothermal energy technology* (MIT-EL 90-001). Massachusetts Institute of Technology. Energy Laboratory. https://dspace.mit.edu/handle/1721.1/60650

Thermal Zones. (2022). *Cotton City Geothermal Lease | 2,501 acres in Hidalgo, N.M. | Established in 1978 | Lightning Dock Geo H1-01 LLC et al. | NMNM 034790*. https://thermalzones.com/claims/nmnm---034790

U.S. BLS. (2021a). *ECI total compensation for private industry workers in utilities*. https://data.bls.gov/timeseries/CIS20144000000000I

U.S. BLS. (2021b). *PPI industry data for electric power generation-utilities*. https://data.bls.gov/timeseries/PCU2211102211104

Winther, J. (2018). *Power production from excess heat in a district heating system* [Masters]. Chalmers University of Technology.

Young, K. R., Levine, A. L., Cook, J. J., Heimiller, D. M., & Ho, J. L. (2019). *GeoVision Analysis Supporting Task Force Report: Barriers. An Analysis of Non-Technical Barriers to Geothermal Deployment and Potential Improvement Scenarios*. National Renewable Energy Lab.(NREL), Golden, CO (United States).